Stabilization of Silicon Surfaces by Thermally Grown Oxides*

By M. M. ATALLA, E. TANNENBAUM and E. J. SCHEIBNER

(Manuscript received January 7, 1959)

A study has been carried out of the stability of silicon surfaces when they are provided with a chemically bound solid-solid interface. Stable surfaces have been obtained with the system silicon-silicon dioxide when the oxide is thermally grown. This latter system has been studied in some detail. In this paper the following phases of our investigation are presented: (i) some aspects of the thermal oxidation process and properties of the oxide; (ii) the electronic properties of the resulting silicon-silicon dioxide interface; (iii) the application of the process to devices and resulting device characteristics.

I. INTRODUCTION

In this introduction we will give a qualitative discussion of the problem of stabilization of semiconductor surfaces.

1.1 *Atomically Clean Surfaces*

Fig. 1(a) is a schematic diagram of a clean [100] silicon surface showing the surface dangling bonds or unfilled orbitals. Since two electrons can occupy a free orbital, surface atoms may become negatively charged, thus acting as acceptor surface states [Fig. 1(b)]. The existence of these states in crystals was first proposed by Tamm,[1] based on a special one-dimensional model. A more general treatment by Shockley[2] showed that surface states can occur only if there is a separate potential trough at the surface or if the energy bands arising from separate atomic levels overlap. He further concluded that surface states should occur in the forbidden gap and their number should be approximately equal to the number of surface atoms.

Experimentally, therefore, one expects to find that an atomically clean

* This work was supported in part by the Department of the Army under Contract DA 36-039 sc-64618.

surface would be strongly p-type, corresponding to a surface state density roughly equal to the density of surface atoms [Fig. 1(c)], and strongly sensitive to surface effects such as chemisorption. Measurements on germanium surfaces prepared by the Farnsworth[3] technique (argon bombardment, then annealing at 500°C in high vacuum), of work function,[4,5,6] photoconductance,[7,8,9,10] surface conductivity[9,10,11] and field effect[7,9,11] have indicated that there is a large density of surface states and that these surface states are the dangling bonds which act as acceptor-type states by trapping bulk electrons and forming a p-type surface. The data also indicate that the adsorption of gases which can bond co-

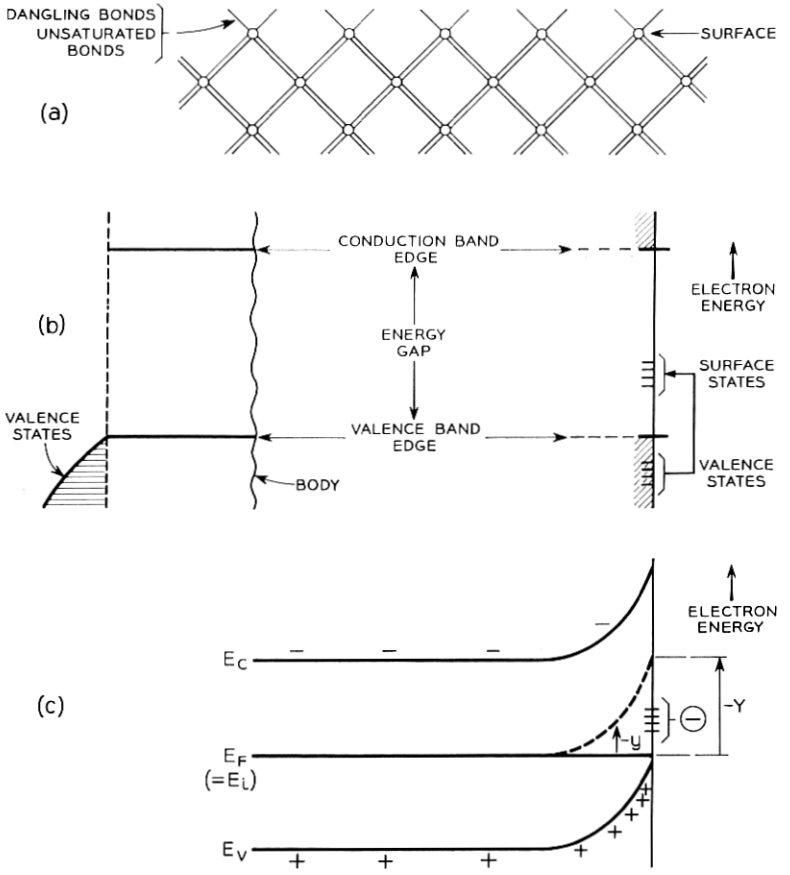

Fig. 1 — (a) Atomic diagram of [100] surface; (b) surface states; (c) resulting band bending near the surface of an atomically clean intrinsic material.

valently with these unfilled orbitals affects the density of surface states and the electrical properties of the surface. More recent measurements,[12] still only preliminary, on cleaved germanium surfaces in high vacuum, appear to be in agreement with those obtained on bombarded and annealed surfaces.

Measurements on atomically clean silicon surfaces are not yet as complete as are those on germanium surfaces. There is strong evidence that clean silicon surfaces are obtainable by high-temperature, high-vacuum heating, as indicated by field emission patterns,[13,14] secondary electron emission[15] and low energy electron diffraction.[16] From the nature of the surface states on germanium surfaces as outlined above, one would expect considerable resemblance between clean germanium surfaces and silicon surfaces.

From the standpoint of device technology, one may expect that truly clean surfaces are not desirable. A junction device would not be operative if its surfaces were atomically cleaned, since the resulting surfaces would be strongly p-type (as present evidence indicates), regardless of the body doping, and a low-resistance surface path would shunt the device.

1.2 *Practical Surfaces*

It is obvious from the above discussion that the usual processes of "surface cleaning" as used in device preparation, such as etches or rinses, do not provide "surface cleaning" in its true sense. A more appropriate term is "surface doping," since such processes generally provide surface structures, complex and unknown, which are found empirically to produce surface properties compatible with the device body properties (through the attainment of a suitable density, distribution and type of surface states, and hence the term surface doping).

Fig. 2(a) shows a possible distribution of surface states on an atomically clean surface. These are all acceptor-type states (neutral when unoccupied, negative when occupied). Chemisorption of some foreign species on the surface may produce the following changes [see Fig. 2(b)]: (a) removal of some of the original acceptor states, (b) introduction of new acceptor and donor states (neutral or positive) and (c) introduction of outer states located beyond the interface, within or on the surface of a grown film. Due to their usually longer relaxation times, these are called "slow" states, in contrast to the interface or "fast" states [see Fig. 2(c)].

For a surface in equilibrium with the body, the potential distribution near the surface is determined by the density, distribution and type of all the surface states. In contrast to the atomically clean surface, which develops a strongly p-type surface conductance [Fig. 1(c)], the surface

conductance of a practical surface may be either p-type or n-type, depending on the existing surface states as determined by surface treatment. This important concept was first appreciated by Bardeen.[17] Fig. 3 illustrates potential distributions at the surfaces of n-type and p-type materials when *donor*-type surface states predominate, hence producing a net positive surface charge which must be compensated by an equal negative charge in a surface space-charge layer.

A point of particular interest and basic significance follows from the above. If a certain surface treatment produces a predominance of either donor- or acceptor-type states (irrespective of body doping), it is evident that the surfaces near the various regions of a device (p and n) can, at best, provide a compromise compatible with the device. For instance, for a p-n junction with predominantly donor-type surface states (net positive charge), the tendency is to make the p-region less p (and possibly inverted), while the n-region becomes more n. For a multiple junction

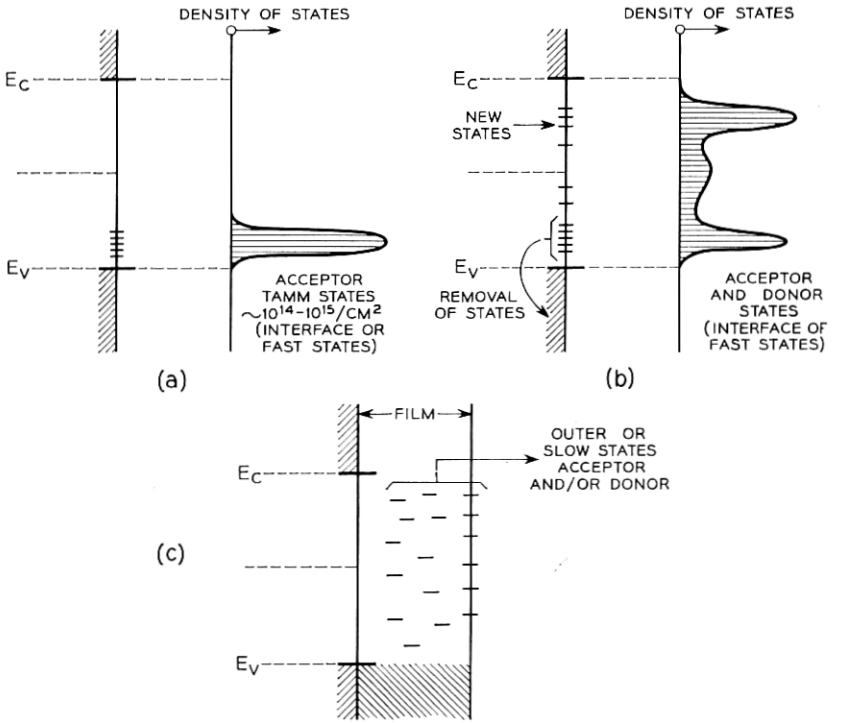

Fig. 2 — (a) Surface states on an atomically clean surface; (b) interface or fast states on a practical surface; (c) outer or slow states on a practical surface.

device it is obvious that the problem of simultaneous compatibility of the surface with the various regions may become quite critical, particularly with high-resistivity materials. This point will be considered in more detail later.

1.3 *Nature of the Surface Stability Problem*

Practical surfaces obtained by the usual empirical techniques involving etches, rinses, etc., are known to show various degrees of instability. They are generally sensitive to various ambients producing drifts in surface properties that are usually not completely reversible. There are at least three main reasons for surface instability:

i. Replacement of interface impurities where an impurity B may replace a previously existing surface impurity A, depending on their relative affinities for the semiconductor. This, in general, will modify the distribution and density of the interface or fast states and, accordingly, the surface potential.

ii. Ionization of adsorbed neutral impurities. This requires both the availability of active sites at the free surface and electronic exchange across a surface film between the adsorbed species and the semiconductor. Depending on its relative electronic affinity, a neutral molecule located at an active surface site (constituting an electronic state) will either re-

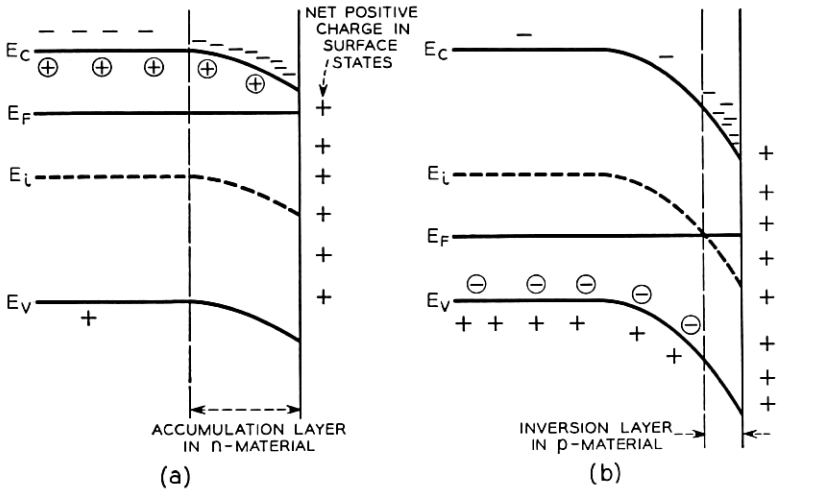

Fig. 3 — Band bending at the surfaces of p and n semiconductors due to surface states that are predominantly donor-type.

ceive an electron from the semiconductor, producing a negative surface charge, or give up an electron to the semiconductor, producing a positive surface charge. Tunneling or direct conduction are probably the mechanisms responsible for the electronic exchange. These (i and ii) are the outer or slow states.

iii. Replacement of these outer impurities may also occur, producing a change in the density, distribution and type of the slow states.

In addition to the above mechanisms, one might also consider a distinctly different process of instability which is generally operative in the vicinity of a junction. Here, surface ions produced by processes other than electronic exchange with the semiconductor, such as hydrolysis, etc., can migrate on the surface under the influence of the fringing field of the junction. A second paper to be published is entirely devoted to a detailed study of this process.

II. TECHNIQUES FOR MEASUREMENT OF SURFACE STATES

In the course of this work several techniques have been used for measuring the detailed surface properties of silicon surfaces, particularly as related to surface states. These included the large-signal ac field effect technique,[18,19] the large-signal ac field effect technique with superimposed dc bias, a zero-frequency four-point probe field effect technique, the surface photovoltage technique[20] and the n-p-n or p-n-p channel technique.[21,22] The majority of the results presented here, however, have been obtained by the field effect techniques. It seems in order, therefore, to present here a brief review of the basic principles and concepts underlying field effect work.

2.1 *Basic Concepts of the Field Effect*

The object of this technique is to determine the density and distribution of surface states. Application of a field transverse to the semiconductor surface produces a change in the band bending near the surface to maintain charge neutrality. This, in effect, alters the location of the Fermi level at the surface and, accordingly, changes the occupancy of the surface states. One measures changes in surface conductance with field (or plate voltage), from which the density and distribution of states are obtained.

2.1.1 *Field Effect with No Surface States*

Fig. 4(a) shows the bands near the surface of an intrinsic semiconductor which are straight in the absence of surface states or charge on the

field plate. The conductance of a region near the surface is due to electrons in the conduction band and an equal number of holes in the valence band. When a voltage is applied to the plate with respect to the semiconductor the bands near the surface must adjust to the point where the net charge in the semiconductor is equal and opposite to that on the plate, Fig. 4(b). If ΔN and ΔP are the changes in the number of electrons and holes per unit area, due to plate charge Q_P per unit area, the corresponding change in surface conductance ΔG is given by

$$\Delta G = q(\mu_n \Delta N + \mu_p \Delta P). \tag{1}$$

One defines the derivative dG/dQ_p, as the "field effect mobility" $\mu_{F.E.}$. It can be shown[18] that ΔG exhibits a minimum value that corresponds to a unique potential distribution near the surface for each body resistivity. For intrinsic material, the bands are bent by an amount $Y = -\ln b$, where $b = \mu_n/\mu_p$. If the bands are so strongly bent in either direction that the number of one type of carrier is negligibly small as compared with the number of the other, then a change in field-plate charge will induce an equal and opposite change in the majority carrier and the field effect mobility approaches the surface mobility of that carrier. Fig. 4(c)

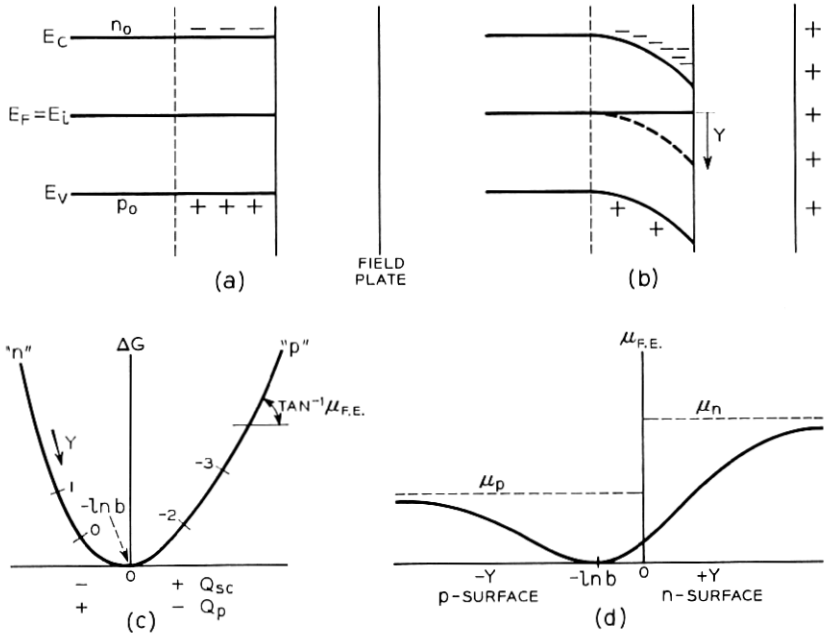

Fig. 4 — Field effect in the absence of surface states.

shows the variation of conductance with plate charge (equal and opposite to space charge Q_{sc}) with the corresponding values of surface potential Y [in $(kt)/q$ units]. In Fig. 4(d) the changes in field effect mobility with surface potential are shown. For any other resistivity one can calculate the variation in surface conductance with charge and the corresponding surface potential using the space-charge equations derived by Garrett and Brattain,[23] which are also conveniently available in graph form.[24] In many cases, one needs to include the effect of surface scattering on carrier mobility. No direct measurements are available, however, and the common practice is to apply Schrieffer's theoretical results.[25]

2.1.2 *Field Effect with Surface States*

In the presence of surface states, part of the charge on the field plate will terminate on charges in surface states. If one now changes the charge by some amount, both the semiconductor space charge and charges in the surface states will change. The resulting change in surface conductance, however, will always be *smaller* than one which would be obtained in the absence of the surface states. The experimentally obtained curve of ΔG versus Q_p is generally wider than that calculated with no surfaces states. Experimentally,[18,19] one varies Q_p at some frequency and observes on an oscilloscope the variation of ΔG versus Q_p . Only states with relaxation times shorter than the period of the frequency used will be effective. Slower states will only contribute a fixed charge.

The point of minimum surface conductance must be obtained in order to provide the reference point for the quantitative evaluation of the results.[18] It has been pointed out in the preceding section that the minimum conductance corresponds to a unique value of the surface potential Y for a given resistivity. Furthermore, the conductance in general is a unique function of Y for each resistivity. Therefore, one adjusts the experimental curve of ΔG versus Q_p with the theoretical space charge curve along the ΔG-axis until the two minima are matched, as shown in Fig. 5. It must be noted that their lateral relative position is arbitrary. Now one transfers the points of various values of Y on the theoretical curve horizontally to the experimental curve, thus providing the value of surface potential at each point on the curve. Furthermore, the horizontal segments between the two curves at each value of Y represent essentially the net charge in surface states Q_{ss} (difference between total charge or plate charge and charge in space charge) with an unknown additive constant. From plots of dQ_{ss}/dY versus Y, one may then fit the results with an approximate distribution of surface states. Rigorously

speaking, an exact distribution is only obtainable if the experiment is carried out throughout the range of $Y = \pm\infty$.[26]

2.1.3 *Effect of Slow States*

If one applies a step voltage to the plate, one will first get a corresponding change in surface conductance resulting from a change in surface potential, in conformity with the fast state occupancy requirements discussed above. If no other states are present, the new value of surface conductance would be maintained indefinitely. However, if slow states are present, their occupancy, which is determined by their location with respect to the Fermi level, must gradually change to correspond to the new equilibrium condition. Since the total charge in the surface states and the space charge must remain constant (equal and opposite to the plate charge), a change in occupancy of the slow states will cause a gradual redistribution of charge in the space-charge region and in the fast surface states. It is obvious that this will always correspond to a *decay* in the initial change in conductance. If the density of the slow states exceeds the plate charge density, the decay is almost complete, with a time constant of the order of the relaxation time of the slow states. *This is evidence of electronic exchange between the semiconductor and the slow or outer states.* The same phenomenon is also observed in three different ways in ac field effect measurements. First, if one superimposes a dc bias on the ac field signal, one observes an immediate shift of the field effect curve towards p or n, depending on the polarity of the dc bias. This is followed by a slow decay towards the initial curve. Release of the dc bias will simply reverse the effect, with a final return to the initial condition. Second, by changing the ambient, one may observe a shift to-

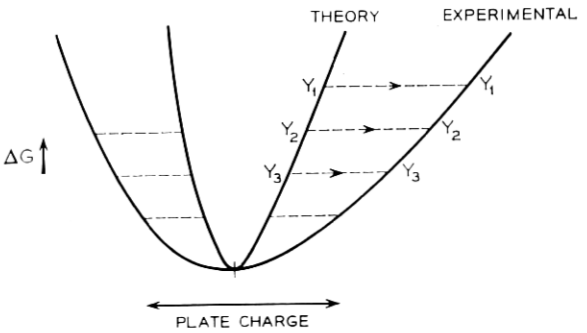

Fig. 5 — Determination of charges in surface states from field effect experiments.

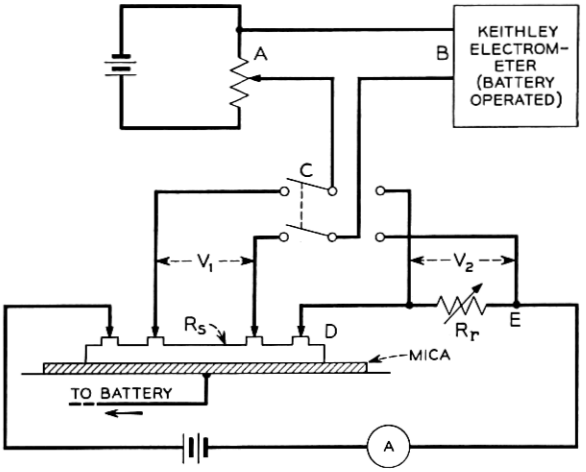

Fig. 6 — Circuit diagram of the zero-frequency four-point probe technique.

wards p or n, depending on the ambient.[27] This is an indication of a change in the density of the slow states and in the magnitude of the fixed charge they represent. It is a further indication of the ionization of neutral adsorbed impurities by electronic exchange with the semiconductor through the surface film. Third, if the frequency of the measurement is reduced to the range of frequencies of the slow states, one observes smaller changes in conductance corresponding to very low field effect mobilities.

2.2 *Zero-Frequency Four-Point Probe Field Effect Technique*

In many cases, particularly for device purposes, one requires a measurement of all the states, fast and slow. This may be done by the ac method, by repeating the measurements at various frequencies. Another alternative is the zero-frequency* four-point probe technique, shown in Fig. 6. The outer electrodes are used to feed in the current and the voltage drop is measured across the inner electrodes. The voltage drop across the specimen is initially balanced against a reference resistor R_r in series with the specimen. The change in conductance ΔG produced by a field is obtained from the voltage difference ΔV between the specimen and the reference resistor, $|V_2 - V_1|$:

$$\Delta G = \frac{\Delta V(L/w)}{I_0 R_s^2} \text{ mhos/}\square, \tag{2}$$

* The term "zero-frequency" is used to distinguish between this method and the conventional dc field effect method used to observe conductivity decay.

where L and w are the length and width of the specimen, I_0 is the current and R_s is the sample resistance. The plate charge is obtained from the voltage applied and the measured capacity of the plate specimen.

2.3 *Characterization of a Surface Treatment*

A complete characterization of a surface is a detailed description of the type, density and distribution of all the surface states. This allows one to predict the surface potential obtained for any resistivity material as a result of these same surface states. In many cases, however, particularly in device applications, it may suffice to know whether a certain surface treatment will or will not produce surface inversion. To extrapolate field effect results obtained on a material of some resistivity to other resistivities, one must show that the surface treatment and the resulting fast surface states are not dependent on concentration and type of body doping.

Fig. 7(a) shows a field effect curve produced at zero-frequency and hence *includes all the states*. Point o corresponds to zero charge on the field plate. Point i corresponds to an intrinsic surface or $Y_i = u_b$, where $u_b = \ln\lambda$ and $\lambda = p_0/n_i$, with p_0 the hole density in the body and n_i the intrinsic density. Fig. 7(b) corresponds to the "onset of surface inversion". To change the surface potential from its initial value Y_0 to the onset of inversion Y_i one must apply a charge $-Q_{0-I}$ to the plate. Invoking the condition of charge neutrality at point i:

$$[Q_{ss}]_I = Q_{0-I} - [Q_{sc}]_I , \tag{3}$$

where Q_{0-I} is measured and $[Q_{sc}]_I$ is calculated for the particular resistivity of the specimen used. This gives $[N_{ss}]_I = [Q_{ss}]_I/q$, the *absolute*

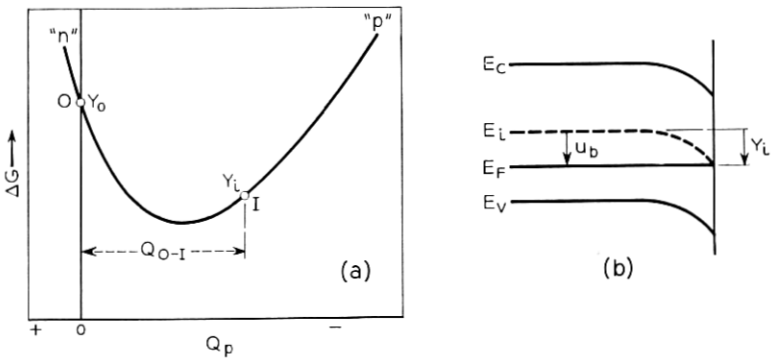

Fig. 7 — Determination of type and strength of surface treatment.

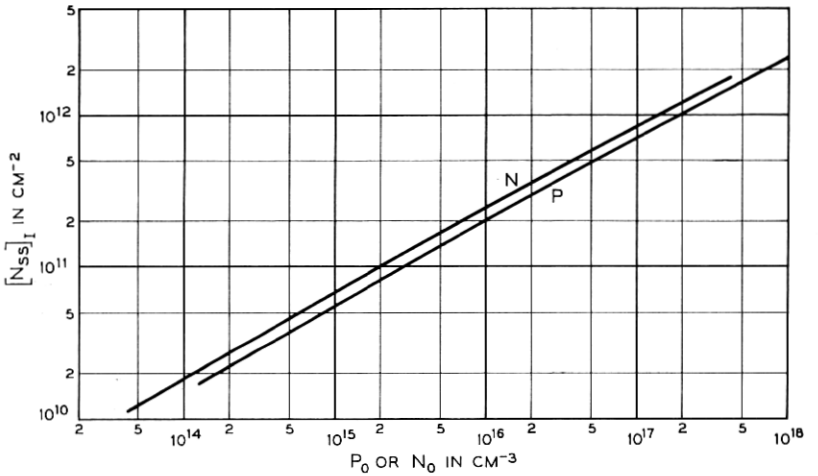

Fig. 8 — Net surface charge required for surface inversion.

number of charges in all the surface states when the Fermi level coincides with the intrinsic level at the surface corresponding to the onset of inversion.

Now, for any doping, the number of charges in the space charge at the onset of inversion is given by[23]

$$(N_{sc})_I = n_i L \left[\lambda(e^{-u_b} - 1) + \frac{1}{\lambda}(e^{u_b} - 1) + \left(\lambda - \frac{1}{\lambda}\right) u_b \right]^{\frac{1}{2}}. \quad (4)$$

Hence, for any resistivity material, the surface states will just bring about the onset of inversion if $(N_{ss})_I$, obtained experimentally, is equal to $(N_{sc})_I$ in (4). For higher resistivity, inversion will occur and, for lower resistivity, inversion will not occur. Fig. 8 is a plot of (4) for both p- and n-type silicon.

The procedure we have used for characterizing the effect of a surface treatment is simply as follows:

i. Determine $[N_{ss}]_I$ from the field effect data as outlined above. If this number is positive, it indicates that inversion will occur on n-type material.

ii. From Fig. 8 determine p_0 or n_0 corresponding to $[N_{ss}]_I$. This determines the limiting resistivity below which inversion will not occur; all materials with resistivities above this value will form inversion layers. Now we will introduce some terminology which concisely describes the properties of an oxidation treatment as related to inversion: *p-type oxides* or *n-type oxides* — this indicates the tendency of the oxidation process to *induce* a p-type surface or an n-type surface, respectively, or to induce

inversion in n-type material or in p-type material, respectively. The *strength of an oxide* is defined as the limiting resistivity above which inversion will occur and below which no inversion will occur. To illustrate, let the oxide be characterized as n-type oxide of strength 10 ohm-cm. This means that this oxide produces sufficient surface states to invert the surface of all p-type material of resistivity above 10 ohm-cms.

III. THE OXIDATION PROCESS

3.1 *Introductory Remarks*

In the search for a coating for stabilization of silicon surfaces, several possibilities were considered. These included two general categories: coatings that are deposited by methods such as dipping, painting or evaporation followed by various processes such as baking, and coatings that are grown from the silicon surface itself. The first category generally suffers from such difficulties as: (a) ionic impurities (remembering that 1/10,000th of a monolayer is sufficient to invert the surface of 1 ohm-cm silicon) which will drift with field, producing device instability; (b) lack of uniformity of chemical bonding (if there is any bonding) at the silicon-film interface, particularly with an ill-defined initial silicon surface; (c) poor structures of the coatings from the standpoint of permeability to various ambients and (d) various incompatibilities such as dielectric strength or coefficients of expansion.

For coatings grown out of the silicon surface, we have restricted our efforts to silicon dioxide. We considered two alternatives: oxides grown anodically in electrolytes and thermally grown oxides. Measurements of their transverse conduction indicated substantial differences. The resistivity of the anodic oxide is of the order of 10^{12} ohm-cm, while that of the thermal oxide (grown at about 1000°C) is of the order of 10^{16}. Furthermore, in the anodic oxides, part of the conduction is due to mobile ionic impurities of the order of 10^{18} per cm^3, while the ionic content of the thermal oxide is less than 10^{14} ions per cm^3.

3.2 *Preoxidation Treatment of Silicon Surfaces*

Preliminary studies, using various silicon diodes, indicated a strong dependence of reverse characteristics on the surface treatment preceding the oxidation process. Impurities left on the surface can be partially maintained at the Si—SiO_2 interface through the oxidation process, and may affect the interface characteristics and the device characteristics. To illustrate, by purposely varying the preoxidation treatment on the

same junctions, it was possible to obtain a range of reverse current of 10^{-10} to 10^{-3} amperes. This work provided an extensive empirical background on the effect of preoxidation treatment and indicated the desirability of obtaining as clean a Si—SiO_2 interface as possible. Accordingly, all the details of the procedure prior to and during the oxidation process were chosen to achieve this objective. A suitable preoxidation process must be capable of: (a) removing surface imperfections, damage, etc.; (b) removing the bulk of organic surface residues (weakly bound); (c) removing chemically bound organic substances; (d) removing metallic impurities and (e) providing in a controlled fashion a lightly oxidized surface prior to thermal oxidation.

3.3 *Monitoring the Preoxidation Process*

In exploring the effects of preoxidation treatments, it appeared desirable to have some simple monitoring technique to indicate qualitatively certain effects of the various treatments on some property of the surface. A technique was used which determined whether the surface was hydrophobic or hydrophilic. The technique is based on the water break and water spray tests, whereby the contact angle of water droplets determines whether the surface is wettable (hydrophilic) or not (hydrophobic). The surface to be examined is dipped in liquid nitrogen for about 10 seconds, then mounted under a high-power microscope (400×) in a closed chamber where wet nitrogen is circulated. One first observes a thin sheet of ice forming uniformly on the surface. After the ice melts, a distinctive pattern of water droplets forms which remains for a few minutes before final evaporation. It has been observed that the shape and size of the droplets and the uniformity of the pattern is sensitive to the surface treatment. This process may be repeated (without re-treating the surface) about five to ten times before observable changes in the pattern start to occur, indicating surface deterioration.

The following is a summary of our observations: (i) A silicon surface that has been freshly etched in HNO_3—HF mixtures is strongly hydrophobic. A typical pattern of this surface as obtained by the "liquid nitrogen test" is shown in Fig. 9(a). The droplet size is of the order of 0.0001 inch. (ii) After the etched surface has been boiled in deionized water for as long as one hour, the surface remains hydrophobic. The size of the droplets, however, may slightly increase. (iii) After having been boiled in organic solvents the surface remains hydrophobic, although the shape and size of the droplets may change, [Fig. 9(b)]. (iv) Boiling in water containing detergents does not produce a hydrophilic surface. (v) When the surface is heated in hot oxidizing agents such as HNO_3 for

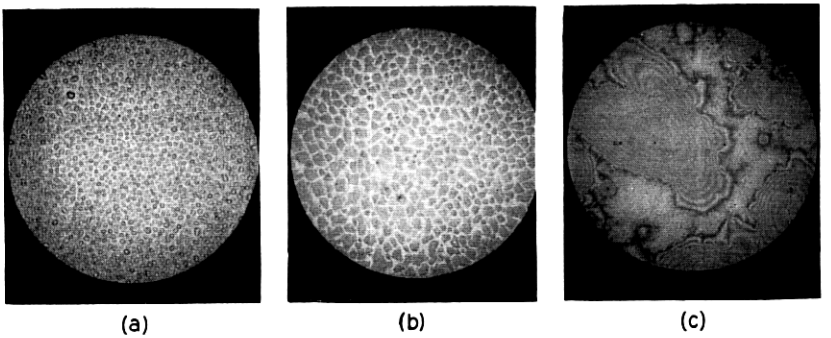

Fig. 9 — Silicon surface examination by the "liquid nitrogen test": (a) after exposure to HF; (b) after subsequent boiling in xylene; (c) after boiling in nitric acid.

10 minutes or more the surface becomes uniformly hydrophilic. Fig. 9(c) shows the optical interference pattern of such a surface just before complete evaporation of the once continuous film of water. (vi) After having been boiled in water this hydrophilic surface remains hydrophilic. (vii) If, however, the hydrophilic surface is exposed for a few seconds to HF vapor, it reverts to a strongly hydrophobic surface. (viii) If the hydrophilic surface obtained by the HNO_3 treatment is exposed to room air, it becomes gradually and nonuniformly hydrophobic. Boiling the exposed surface in water or organic solvents will not restore the surface to its former hydrophilic state. (ix) A thermally oxidized surface is hydrophilic, and shows similar behavior to the nonoxidized one when treated with HNO_3 exposed to room air. A major difference, however, is that its original hydrophilic state can be largely restored simply by rinsing in an organic solvent. This suggests the relative inertness of an oxidized surface compared to a freshly etched surface.

3.4 *The Thermal Oxidation Process and Properties of the Thermal Oxide*

Silicon surfaces were oxidized at temperatures in the vicinity of 1000°C and at atmospheric pressure in both dry and wet oxygen. The oxidation rates in oxygen and in water vapor have been measured[28] using a vacuum microbalance technique. For the range of film thicknesses of about a hundred to thousands of angstroms the oxidation process follows the following parabolic laws:

$$O_2: \quad X^2 = 8.4 \times 10^{10}\, p^{4/5} t\, e^{(-1.7q)/KT}, \tag{5}$$

$$H_2O: \quad X^2 = 2.54 \times 10^{13}\, p^{8/5} t\, e^{(-1.7q)/KT}, \tag{6}$$

where k is the Boltzman constant, T the absolute temperature, X the film thickness in angstroms, p the pressure in atmospheres, t the time in minutes and q the electronic charge. It is of particular interest to note that the activation energies are equal for both O_2 and H_2O oxidation, suggesting that the two types of oxides have the same structure. The high activation energy of 1.7 electron volts is also significant, since it presumably corresponds to extraction of silicon from the lattice and its diffusion in the oxide network.

The following are some properties of the thermal oxide:

i. Electron diffraction studies of thermally grown silicon oxides have indicated no crystalline structure. The film is essentially continuous and amorphous.

ii. The dielectric constant of the film is about 4. It has a resistivity of about 10^{16} ohm-cm, measured in a transverse direction to the oxidized surface. The dielectric strength of the film is between 5 and 10×10^6 volt/cm.

iii. If the surface impurities are not carefully removed prior to oxidation, oxide crystallites will form on the surface that become visible under the microscope if the film grown is of sufficient thickness. This provides rather serious discontinuities in the film.

iv. Discontinuities in the film are also observed at some surface imperfections, due either to the nonuniform growth of the oxide at the imperfection or to impurities trapped at the imperfection and subsequently

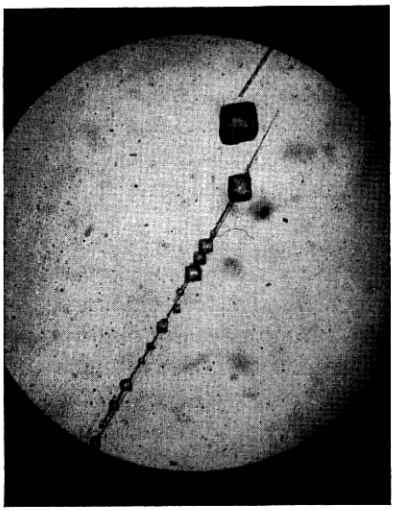

Fig. 10 — Oxide imperfections as revealed by the hot chlorine technique.

affecting the local oxidation. These local imperfections are made beautifully visible, even for films a few atomic layers thick, by the "*chlorine etching*" technique. At a temperature of about 900°C, chlorine gas will etch silicon at a rate of the order of 0.001 inch per minute but will not react with silicon dioxide. To test for film imperfections, the oxidized specimen is placed in the chlorine oven for a few minutes, allowing the chlorine to etch through discontinuities in the oxide. Fig. 10 shows a chlorine-treated oxide surface indicating some imperfections along well-defined surface damage.

v. Uniform oxides have been obtained consistently. They showed few imperfections as indicated by the chlorine test. Oxidized surfaces stored for more than 12 months before exposure to the chlorine test have indicated the permanence of film uniformity. Furthermore, oxidized devices given the 900°C chlorine test indicated no change in their electrical characteristics.

IV. Field Effect Measurements on Thermally Oxidized Silicon:

Both the large-signal ac field effect technique, using a frequency of 40 to 500 cps, and the zero-frequency four-point probe field effect technique were used. The sample resistivities ranged from 80 to several hundred ohm-cms, both for p-type and n-type silicon. Pulled crystals, rotated and nonrotated, as well as floating-zone crystals were used.

4.1 *Evidence for the Absence of Slow States*

Fig. 11(a) shows the ac field effect pattern obtained at 70 cps for a 300-ohm-cm p-type pulled crystal with an oxide thickness of about 500

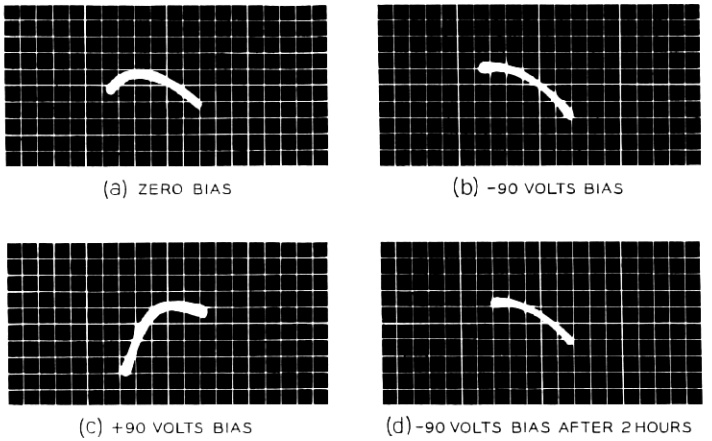

Fig. 11 — Large-signal ac field effect — effect of a superimposed dc bias.

angstroms. The field-plate signal was ±280 volts. For an etched silicon surface, if one superimposed a dc bias on the ac signal, the pattern would shift to one side or the other, then drift back within about a minute to the initial pattern. For the oxidized silicon, however, an application of −90 dc volts produced the shift indicated in Fig. 11(b) and +90 volts produced the shift indicated in Fig. 11(c), all figures having the same calibrations. If one superimposes all three curves, one finds that the actual measured shift of the curves corresponds closely to the 90 volts which have been applied. *This indicates that the usual slow states observed on unoxidized surfaces have been virtually eliminated.* Furthermore, the −90 volts dc bias was left on for two hours with no change in the field effect pattern, which is shown in Fig. 11(d) at the end of two hours. To determine the possible existence of slower states, we have also maintained a dc field in a four-point probe experiment (discussed in a later section) for over 3000 hours with no measurable decay in surface conductance.

To explore the possibility of states with relaxation times corresponding to higher frequencies than the 70 cps used above, a frequency run was performed. This was done on a 300-ohm-cm p-type rotated crystal with an oxide thickness of 180 angstroms. The field effect pattern was ob-

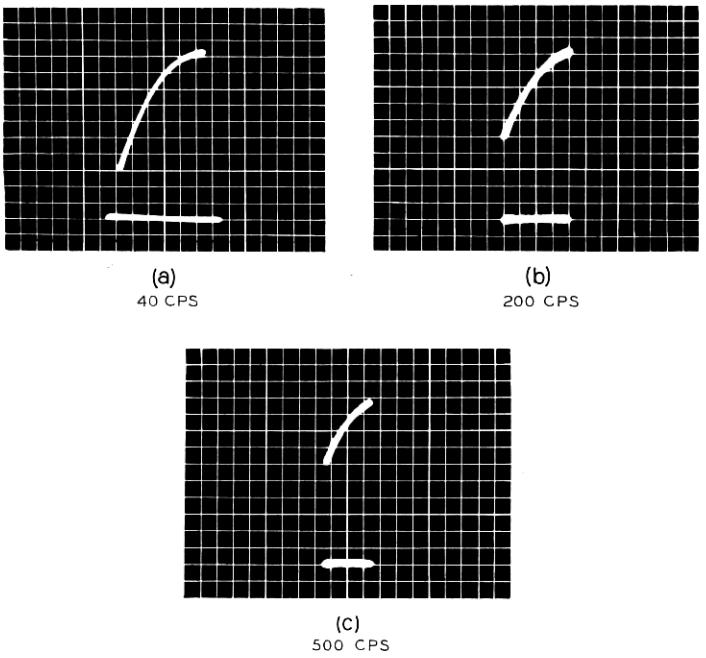

Fig. 12 — Large-signal ac field effect — effect of frequency.

served at 11 different frequencies from 40 to 500 cps. Fig. 12 shows the patterns obtained at 40, 200 and 500 cps, all drawn to the same scales. Due to distortions at the higher frequencies, lower plate voltages had to be applied at 200 and 500 cps. Here again, if one superimposes all three patterns by making the midpoints coincide, one obtains *one identical curve*. This shows that no slow states (or not-so-slow states) are observable up to 500 cps. Unfortunately, our measuring set is limited to 500 cps and, accordingly, we have no knowledge of the lower limit of the relaxation time of the surface states.

4.2 *Effect of Ambients*

The experiments reported in the above section were performed in dry oxygen. To study the effects of ambients, the following gases have been circulated: dry oxygen, dry nitrogen, wet oxygen and wet nitrogen (~40 per cent relative humidity), ammonia and ozone. No shifts in the field effect pattern were observed over several hours. On replacing the oxidized sample with etched silicon and germanium samples, shifts in the field effect patterns were observed in accordance with the usual experience.

4.3 *Effect of Presence of External Impurities During Oxidation — Not-So-Fast States*

This effect was first observed accidentally when the oxidation tube was cracked and impurities from the heating elements of the oven were present during the oxidation process. The general effect is to produce "*not-so-fast states*," as indicated by both the zero-frequency technique and the ac technique. The zero-frequency technique indicates a very small change in conductance with applied field. The ac field effect technique, however, by simple changes of the frequency, shows the effects of the not-so-fast states. Fig. 13 shows the results obtained from a sample

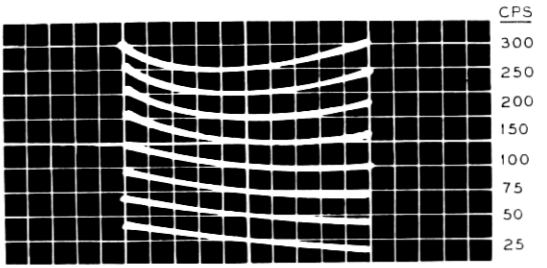

Fig. 13 — Large-signal ac field effect — effect of frequency when not-so-fast states are present.

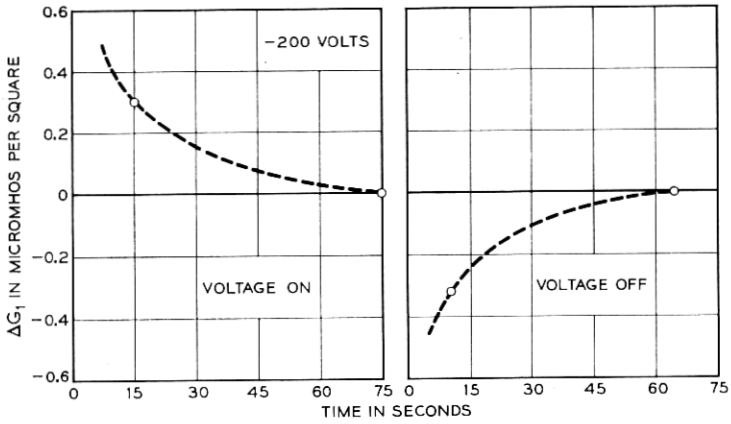

Fig. 14 — Zero-frequency four-point probe field effect — etched silicon surface.

showing this effect. From bottom to top the frequencies are 25, 50, 75, 100, 150, 200, 250 and 300 cps. As shown, the tendency is for the surface to become more p-type with increased frequency, indicating that the responsible states are mainly donor type (neutral or positive). It is of further interest to note that most of the change in the pattern occurred between 50 and 300 cps, setting a range of relaxation times for these states between 3 and 20 milliseconds.

4.4 *Zero-Frequency Field Effect Measurements on Oxidized Floating-Zone Silicon*

First we will demonstrate the typical behavior of etched silicon surfaces when they are examined by the zero-frequency four-point probe technique. Fig. 14 shows, for a p-type silicon specimen, a typical decay with time of surface conductance of 180 ohm-cm produced by the floating-zone technique.* The change in conductance decays to practically zero in a little over one minute. The plate voltage was −200 volts, corresponding to a plate electronic charge density of $7 \times 10^{10}/cm^2$. On removal of the plate voltage, the reverse effect is obtained.

Samples of the same crystal were oxidized to various oxide thicknesses. The field effect results were quite reproducible for each sample and from sample to sample. In all cases, no decay in the change in conductance was observed. Fig. 15 shows the results from one unit, plotted as the change in surface conductance versus plate charge. The calculated space

* These samples had 22 zone passes in a hydrogen atmosphere. It is believed that most fast-diffusing impurities, as well as oxygen, have been removed.

charge plot is also shown, from which the values of surface potential were obtained. They are shown on the experimental curve. Note that, with this technique, the *lateral location of the theoretical space-charge curve is absolute.* The horizontal segments between the theoretical and the experimental curves represent the total net charge in surface states (and also fixed charges if present — which is not the case, as will be shown shortly from data on the effect of time). The point of intersection corresponds to zero net charge in the surface states; to the right, there is a net positive charge and, to the left, a net negative charge. From this, it is concluded that *the surface states present are of two types, donor and acceptor.* By analyzing the data in the usual way, the following approximate distribution of states was obtained:

i. An acceptor level located at about 0.4 electron volt below the intrinsic level of density of the order of $10^{11}/cm^2$.

ii. A donor level located higher than 0.3 electron volt above the intrinsic level of density of the order of $10^{10}/cm^2$.

iii. A nonuniform and less significant distribution near the center of the band of average density of the order of $10^9/cm^2$ volt.

For this high-purity floating-zone material, *the general tendency after*

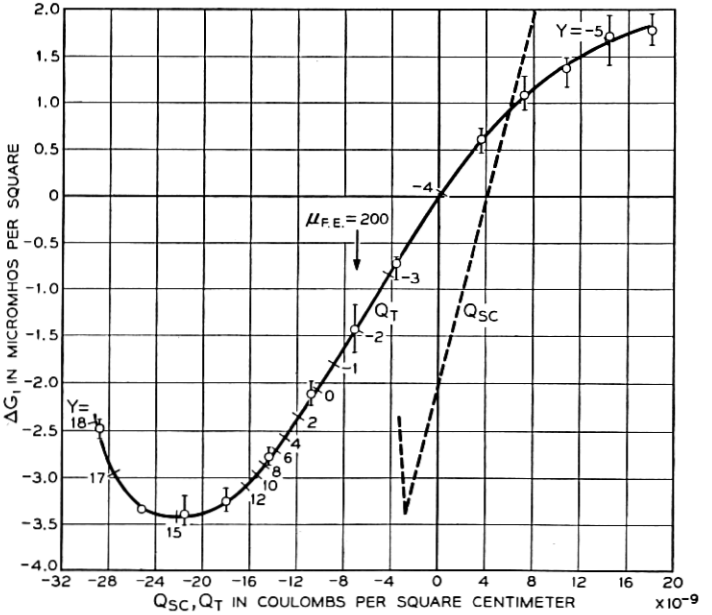

Fig. 15 — Zero-frequency four-point probe field effect — thermally oxidized high purity p-type crystal.

oxidation is to produce a p-type surface, indicating the predominance of the acceptor-type surface states. In terms of oxide type and strength, discussed previously, these results indicate a p-type oxide of strength of about 3 ohm-cm; i.e., the same surface states would invert all n-type silicon surfaces with resistivities above 3 ohm-cms.

To determine whether there is any significant number of *very slow states* within or on the surface of the oxide, a sample was given a life test in which, after its field effect characteristics were measured, a dc bias of 400 volts was left on (corresponding to a plate electronic charge of about $1.5 \times 10^{11}/\text{cm}^2$). Periodically, the surface conductance was remeasured and the field effect curve was re-obtained. The test has so far exceeded 3000 hours with no detectable change in the conductance or the field effect curve. Since the film dielectric constant and resistivity are 4 and 10^{16} ohm-cms, respectively, its relaxation time $\kappa\rho/4\pi$ (in electrostatic units) is of the order of one hour. One concludes, therefore, that *the number of outer or very slow states is insignificantly small.*

4.5 *Surface Properties of Oxidized Silicon Pulled Crystals; Effect of Body Impurities*

Field effect experiments have also been performed on more than 20 samples from a number of high-resistivity pulled crystals, nonrotated and rotated at different rates during growth. They generally exhibited, when oxidized, the same general behavior as far as the absence of slow states, high field effect mobility, and insensitivity to ambients. One very significant difference that was observed, however, was that *the surfaces obtained were generally n-type;* i.e., *the oxides were n-type and had a wide range of strength from 0.5 to 20 ohm cms.* This indicates that, in contrast to high-purity floating-zone crystals, the donor-type surface states are more predominant than the acceptor-type states. The variations in film strength were observed both from crystal to crystal and from sample to sample in the same crystal. In many cases, the surface was so strongly n-type that no conductivity minimum was observed even when a plate signal corresponding to about 2×10^{11} electron charges per cm^2 was applied, indicating a density of donor-type states in excess of this figure. To show that the n-type surface was *induced* by charges in surface states rather than by some body doping in a small region near the surface, the oxides were removed by exposure to HF vapor for 30 seconds, followed by a water rinse. Thermal probing of the surface indicated p-type material, and ac field effect observations indicated the disappearance of the initial n-type surface.

In view of the above results on the high-purity crystal, it was further

concluded that a strong n-type surface, as is obtained with pulled crystals, is *not* a characteristic behavior of thermally grown silicon oxide. To explain this behavior of pulled crystals, the main remaining possibility is crystal impurities, particularly the fast diffusants. This possibility has been supported by two main observations:

i. Pulled n-type crystals have shown, in the majority of cases, rather large increases in body resistivities during the oxidation process (as high as two orders of magnitude). These were observed when the samples were quenched from the oxidation temperature to room temperature. This change, however, will decay at room temperature, and the decay is nearly complete in the order of an hour. At 200°C the decay is complete in less than 10 minutes. This phenomenon is not understood, but it is presumably due to some body impurities producing donor-type levels,[29] possibly through formation of complexes with oxygen in the crystal or precipitation of acceptors.[30] In our work with high-purity floating-zone crystals, on the other hand, these changes in body resistivity were either absent or comparatively small, the largest observed increase being about 15 per cent. Therefore, it seems quite plausible that the source of the high density of donor-type surface states observed with pulled crystals is fast-diffusing body impurities which are gettered by the oxide.

ii. The second observation was a result of the following experiment. A 10,000-angstrom gold film was evaporated on the same high-purity floating-zone sample for which results were given in Fig. 15. The sample was then heated in an argon oven for 30 minutes at 950°C. The excess gold was then removed and the sample re-etched. From the increase in resistivity it was estimated that approximately 3×10^{14} atoms/cm^3 of gold were added. This is based on published data[31,32] on the donor and acceptor levels introduced by gold in silicon (donor level 0.35 electron volt from valence band; acceptor level 0.54 electron volt from conduction band), and on the assumption that each gold atom is electrically active. The sample was oxidized (300 angstroms) and the zero-frequency field effect measurement was repeated. The results are shown in Fig. 16. One now finds that the surface is *n-type*, the conductivity minimum is barely observed and the field effect mobility has decreased markedly to about 80 cm^2/volt-sec. The oxide was then removed by HF vapor, followed by a water rinse, and the surface reverted to p-type. From this, one concludes that added body impurities such as gold (and possibly others that were unknowingly introduced into the crystal along with the gold), can diffuse to the surface and produce donor-type surface states that will induce a strong n-type surface. Finally, to determine the effectiveness of the oxide in gettering body impurities, the same sample was re-oxidized

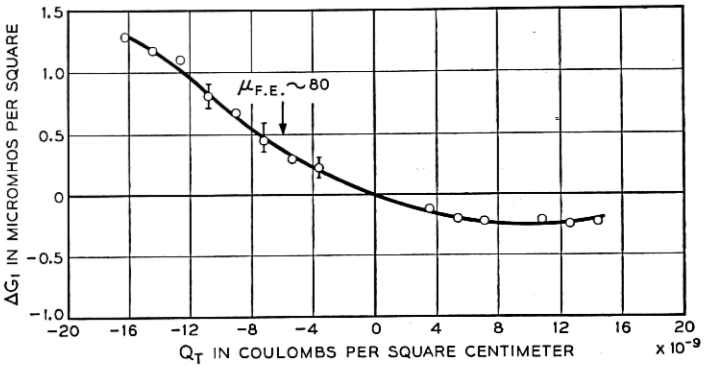

Fig. 16 — Zero-frequency four-point probe field effect — effect of adding gold to crystal.

for 65 hours at 920°C (4000 angstroms), the oxide was removed and a one-half-hour oxide was regrown (300 angstroms). Field effect measurements were made and are presented in Fig. 17. Comparing this with Figs. 15 and 16, one finds the resulting surface *still n-type*, yet the field effect mobility is slightly higher and the conductance minimum is more pronounced. From body resistivity measurements, one calculates a decrease in gold content from the initial concentration of 3×10^{14} to 1×10^{14} atoms/cm^3.

4.6 *Comment on the Nature of Surface States at an Oxidized Surface*

It was pointed out in the introduction that surface states exist on an atomically clean surface. These are associated with the dangling bonds

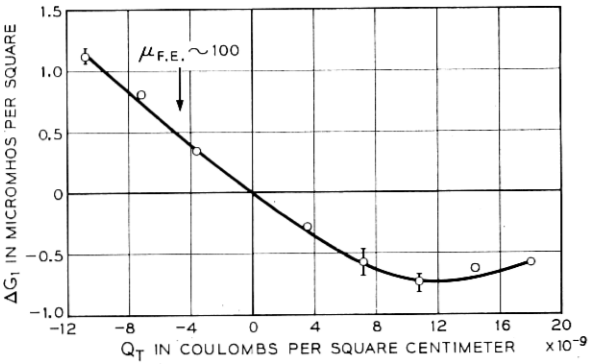

Fig. 17 — Zero-frequency four-point probe field effect — gold gettering by prolonged oxidation.

or free orbitals. These "Tamm" states are acceptor-type states which are neutral when unoccupied and negatively charged when occupied. It has further been shown, theoretically,[33] that, at the interface between two dissimilar crystals, Tamm-type states will also exist. In the case of a thermally grown oxide on a silicon surface, one may visualize a *gradual* transition in structure (within a few atomic layers) from an all-crystalline structure to an all-amorphous structure. The composition must also undergo a gradual transition from all silicon to all silicon dioxide. One intuitively expects, therefore, that such a transition should give rise to some Tamm-type surface states, as well as states associated with vacancies due to lattice mismatch. For the surface states observed in our experiments with thermally oxidized surfaces, we propose the following tentative model. The acceptor-type states observed are Tamm-type states and vacancy states, while the donor-type states observed are associated with impurities that may be introduced in a variety of ways. From this, the concepts result of surface doping and surface-state compensation, in exact analogy to their counterparts in the body of a semiconductor. For further examination of this model, it appears quite important to study the surface states on an atomically clean silicon surface which has been thermally oxidized in pure oxygen. This study is currently in progress.

V. CHARACTERISTICS OF THERMALLY OXIDIZED DEVICES

5.1 *Characteristics of Oxidized Diodes*

The oxidation process has been applied to several thousand diffused junctions. These included n^+-p and p^+-n diodes (graded junctions) in the range of breakdown voltages of 20 to 400 volts, n-p-n and p-n-p structures and p-n-p-n switching transistor structures. Crystals used were all pulled crystals, with phosphorus and boron the doping impurities.

The following results were all obtained on junctions with thin oxide films, 150 to 300 angstroms, prepared at 920°C in dry oxygen (10 to 30 minutes oxidation time). After oxidation the junctions were quenched in room air. No special precautions were taken for their storage; they were usually stored in plastic boxes in room air. Units stored in this fashion for as long as 15 months have shown no change in electrical characteristics. Most of the measurements given below were obtained in room air, and contacts were made by a point pressed on the top surface of the device. By applying a sufficiently high voltage it is possible to break through the oxide film (only for the thin films) and obtain satisfactory contact for reverse bias current measurements.

Fig. 18 shows the reverse V-I characteristics for two different boron-doped crystals A and B. The junctions were obtained by diffusing phosphorus into a mechanically polished surface, giving a junction which is about 0.001 inch deep. The structure is essentially n^+-p. Each slice had 12 individual diodes 0.025×0.025 inch, and slices A and B had body breakdown voltages of 36.5 and 43 volts, respectively. The circles indicate the average current for each voltage; the range is also indicated. It is seen that the spread is within a factor of 2 to 3, which has been typical for all our results within one slice and within various slices with the same history. From crystal to crystal, however, and sometimes from one diffusion run to another, the reverse currents may vary by one to two orders of magnitude. This is illustrated in Fig. 18. This figure also indicates another significant effect that has been consistently observed with n^+-p

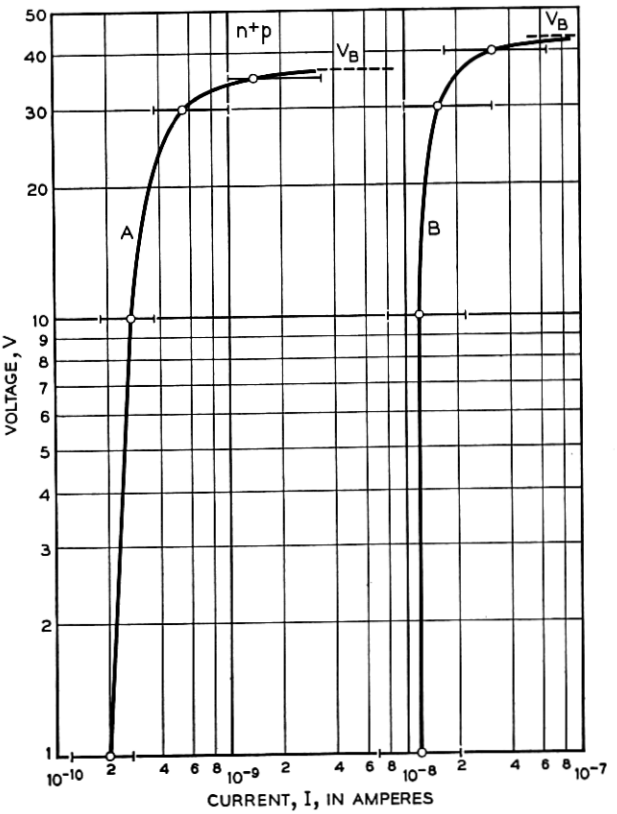

Fig. 18 — Typical characteristics of oxidized n^+-p graded junction silicon diodes.

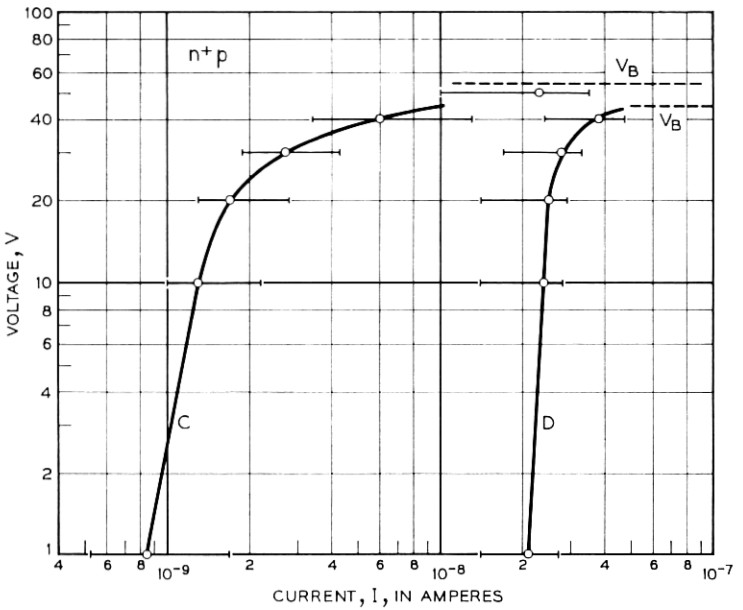

Fig. 19 — Typical characteristics of oxidized n^+-p graded junction silicon diodes.

diodes. *For junctions giving higher reverse currents, there is less dependence of current on voltage.* In general, we have observed that *for n^+p graded junctions the reverse current is proportional to the applied voltage raised to a power which varies from nearly zero to one-third.* Crystal A in Fig. 18 gave a power of 0.11 to 0.18 (in the range 1 to 10 volts). Fig. 19 shows the same effects for two other sets of n^+-p diodes made from two different crystals, with higher body breakdown voltage as indicated. For set C the power dependence varied from 0.14 to 0.28.

From measurements of lifetime by the injection-extraction technique,[34] it was shown that the body saturation current (due to diffusion according to the simple diode theory[35]) is negligible. The contribution of body current to the observed currents must, therefore, be due to space-charge generation.[36,37,38] For graded junctions as used above, however, the space-charge generation current is proportional to the applied voltage (plus a built-in voltage) to the one-third power. Occasionally, this dependence has been observed with oxidized units, but, in most cases, the dependence observed is weaker for n^+-p junctions, as discussed above. This strongly suggests a separate contribution of the surface to the observed currents.

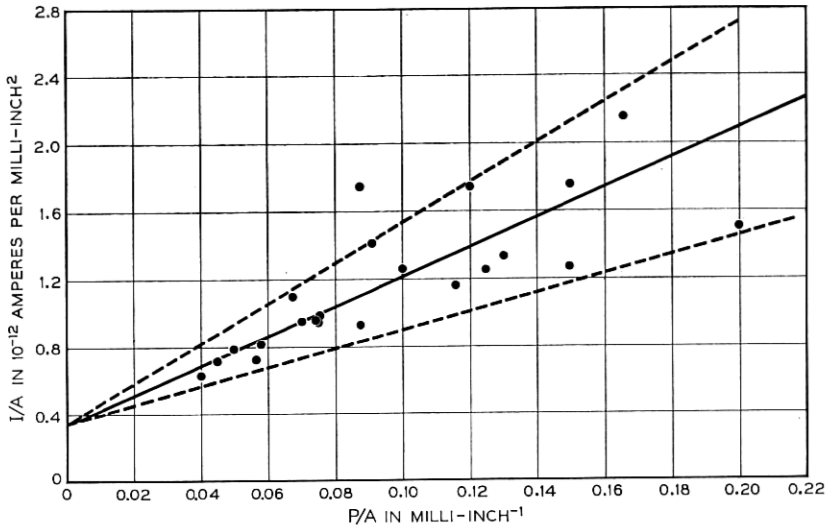

Fig. 20 — Separation of body and surface currents for oxidized diodes.

To illustrate this, the following experiment was performed. On one slice of diffused n^+-p material, 22 rectangular or square units of different sizes were etched and oxidized to a thickness of about 200 angstroms. The range of perimeter to area ratio obtained was 40 to 200 $inch^{-1}$. This is based on the nominal dimensions rather than the actual dimensions, including perimeter irregularities, resulting from etching, and accounts for some of the spread of the data shown in Fig. 20. This figure is a plot of the I/A versus P/A, where I is the reverse current measured at 10 volts, A is the nominal area of the diode and P is its nominal perimeter. If the currents observed were only body currents, this plot would be a horizontal line, indicating that the current density is constant, regardless of shape or size of the diode. One observes, however, that the experimental points have a definite trend towards an increase in I/A with an increase in the P/A ratio. The median line is shown, together with two other lines that contain all the points except one. From the intercepts and slopes, one finds that the currents observed can be split into body and surface components. From Fig. 20, the body component is 5.3×10^{-8} amperes/cm^2 and the surface component is $3.5 \times 10^{-9} \pm 40$ per cent amperes/cm, both measured at 10 volts (for a 40-volt breakdown voltage n^+-p diode) and at 25°C.

For further identification of the mechanisms of the body and surface currents, one must repeat the above experiments at various tempera-

tures and examine the activation energy in different temperature ranges. Preliminary results indicate that, between room temperature and 250°C, the activation energy increases with temperature, approaching approximately 1 electron volt near 160°C and *in some cases* being as low as 0.55 electron volt at room temperature. Tentatively, this suggests that reverse currents near room temperature are due to space-charge generation by traps located approximately at the middle of the energy gap, and that, at higher temperatures, the usual saturation currents due to diffusion will predominate (activation energy equal to the energy gap).

Now, returning to Figs. 18 and 19, one must explain why the dependence of current on voltage is to a power less than one-third. This may be explained in terms of our results from field effect measurements on pulled crystals, as reported in previous sections. It was pointed out that, for pulled crystals, the general tendency is to form n-type oxides, i.e., oxides with a predominance of donor-type states which may invert the surface of a p-type crystal. This means that a "channel" can form on the p-side of an n^+-p diode. The surface component of the observed current, therefore, corresponds to this channel current. Now, if sufficiently high voltage is applied, the channel will "pinch off" and its current will essentially *saturate*. This current, added to the body current which varies as $V^{\frac{1}{2}}$, gives the total current, which will appear to have a weaker dependence on voltage. The stronger the channel formed, the higher its pinch-off current will be and the voltage dependence of the total current above pinch-off voltage will get weaker. For the results of Figs. 18 and 19, this suggests that the pinch-off voltages were below one volt, the lowest voltage used in these experiments. More recent work on n-p-n structures, whereby similar channels were formed by oxidation and the channel characteristics obtained both *before* and *after* pinch-off, substantiates the above explanation.

The above reasoning suggests that one should obtain a markedly different behavior for p^+-n structures. This is, indeed, the case, and Figs. 21 and 22 show typical reverse characteristics of two different samples, E and F, of p^+-n diodes. The junction depth is about 0.001 inch, and the body breakdown voltages are 64 and 32.5 volts for samples E and F, respectively. Sample E consists of 12 diodes and sample F consists of 7 diodes. In the range of 1 to 10 volts, the current is proportional to the voltage raised to a power of 0.4 to 0.64, which is *in excess* of the one-third power expected for a graded junction on the basis of space-charge generation. This, again, is due to surface contribution, which is explainable in the same way we have explained the behavior of n^+-p junctions. The oxide is n-type, which tends to form an *enhancement* or *enrichment* layer

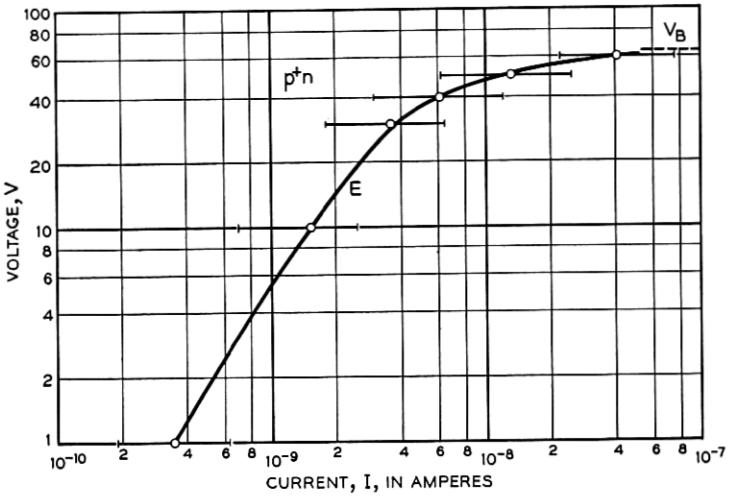

Fig. 21 — Typical characteristics of oxidized p^+-n graded junction silicon diodes.

on the n-region of the p^+-n junction. If this enhancement is not sufficiently strong, one obtains softer reverse characteristics, as shown in Figs. 21 and 22. It is believed that this soft characteristic is made up of a succession of small localized surface breakdowns which occur at various voltages below body breakdown. We have seen cases where, instead of a gradual softness, the reverse characteristic is made up of a succession of distinct segments starting at some low voltage and proceeding until body breakdown is reached. The slopes of these lines correspond to resistances of the order of several thousand ohms. This suggests localized surface breakdowns. These effects are now being studied for shallow junctions (of the order of a micron), using the light emission technique.[39,40] Preliminary results indicate that the occurrence of each of these segments (or knees on the *V-I* curve) corresponds exactly to the onset of light emission (white light from one point on the junction surface).

5.2 *Characteristics of Oxidized p-n-p-n Diodes*

Another device that was oxidized was the two-terminal p-n-p-n structure transistor switch, which is an all-diffused diode with junction spacings of the order of 0.0001 inch. Fig. 23 shows typical characteristics of a set of 20 units processed on one slice, including the high impedance characteristics in both directions. (All these units had a 300-angstrom oxide.) The circles represent the average readings and the corresponding spreads are indicated.

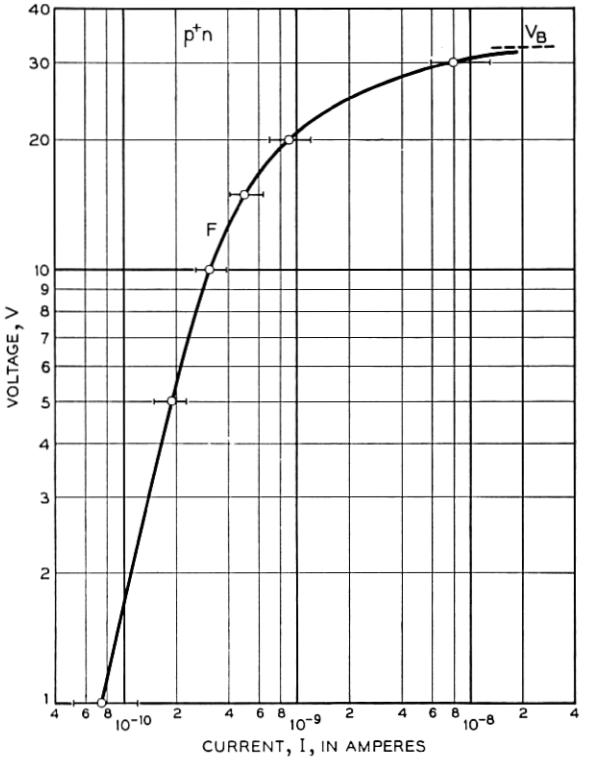

Fig. 22 — Typical characteristics of oxidized p^+-n graded junction silicon diodes.

In this device, as well as in various others, it is important to maintain the lifetime in the oxidation process. For a switching diode, the lifetime will be mainly reflected in the turn-on current of the device. This requirement is compatible with the oxidation process, provided that the cooling after oxidation is controlled. It was possible to maintain the life time, or even show some improvement, by cooling the oxidation oven at a rate of a few degrees per minute. This was checked on both diodes, using the injection-extraction technique for lifetime measurement, and on the p-n-p-n switch, as reflected in its turn-on current.

VI. NOISE IN OXIDIZED DIODES

Excess noise in single-crystal filaments[41,42] and diodes[43] usually exhibits a $1/f^{\alpha}$ spectrum ($\alpha \sim 1$) and is sensitive to surface conditions. Several theories[43,44,45,46] have been proposed to explain this frequency dependence. McWhorter,[43] for instance, suggests that the $1/f$ noise is caused

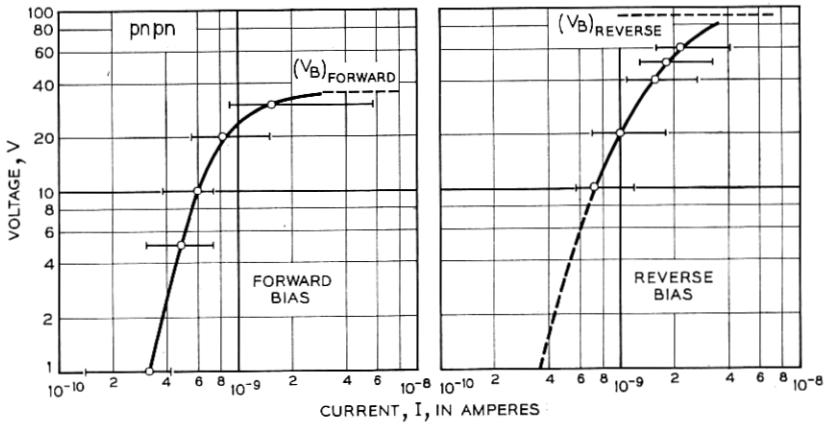

Fig. 23. Typical characteristics of oxidized p-n-p-n silicon switching diodes.

primarily by fluctuations in the occupancy of slow surface states. From field effect measurements as a function of frequency he has deduced a distribution of the relaxation times for the slow states on germanium surfaces, and he has shown that the same distribution can account for the $1/f$ dependence of excess noise. For single-crystal filaments, the fluctuating occupancy of slow states produces conductivity modulation in the bulk. In diodes and transistors, it also modulates the recombination rate at the surface, because of the relation between surface recombination velocity and surface potential.[47]

As discussed previously, thermally oxidized silicon surfaces show no

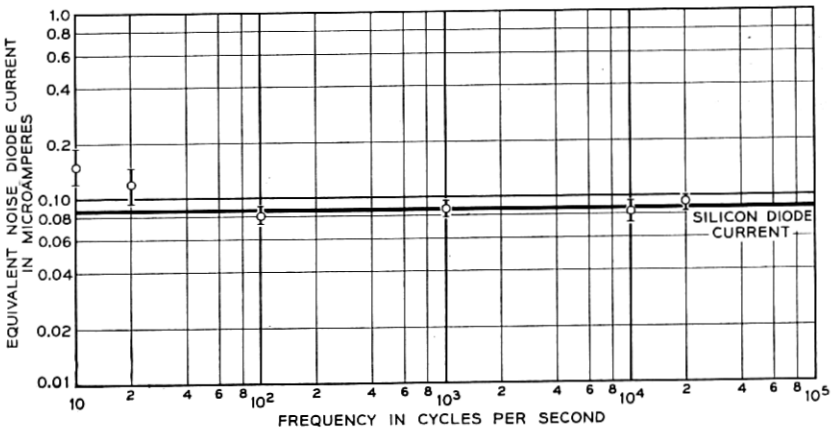

Fig. 24 — Noise in a thermally oxidized silicon diode.

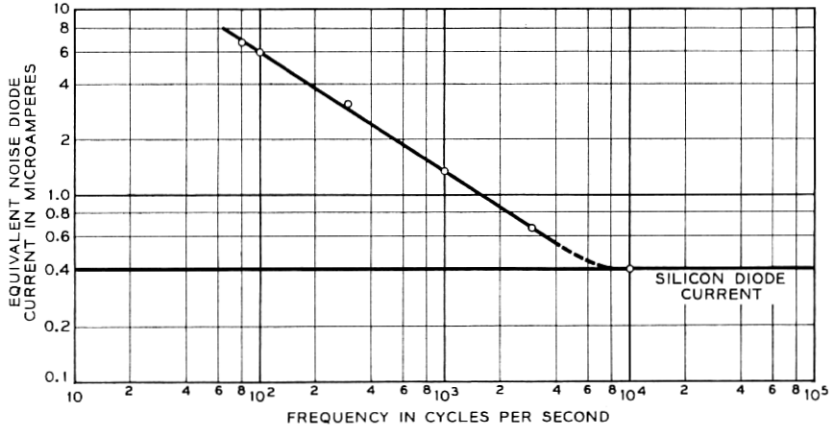

Fig. 25 — Noise in silicon diode after removal of oxide and light etching.

effects of slow states, so that it is of interest to determine whether the $1/f$ noise also is absent. Preliminary measurements of excess noise in oxidized silicon diodes have shown the following:

i. Reverse-biased diodes operated at 75°C in dry air show no noise in excess of shot noise to frequencies as low as 30 cps (Fig. 24).

ii. Removal of the oxide in HF vapor generally does not introduce any additional noise.

iii. After a light etching in an HF-HNO_3 solution a $1/f^{0.65}$ dependence of excess noise was found up to a frequency of about 10 kc (Fig. 25).

VII. SUMMARY

The problem has been re-examined of the stabilization of silicon surfaces when the silicon surface is chemically bound to an appropriate solid film that is well defined in composition and structure. We have studied one such system, namely, the silicon-silicon dioxide system when the oxide film was produced by high temperature oxidation of the silicon surfaces.

i. *Film properties.* The films produced were amorphous, continuous and uniform. Various thicknesses were studied from a few hundred angstroms to tens of thousands of angstroms. The films had a resistivity of about 10^{16} ohm-cm, dielectric constant of about 4, and dielectric strength of about 10^7 volts/cm. The concentration of impurities which were detected as mobile ionic charges were less than $10^{14}/cm^3$.

ii. *Interface properties.* A completely new kind of surface was produced by thermal oxidation, with its own characteristic distribution of surface states. These were fast or interface states; slow or outer states were not

observed. The $1/f$ noise commonly associated with fluctuations in slow states was also not observed down to a frequency of 30 cps. The fast states consisted of both donor-type and acceptor-type states. Their densities and distributions, which determine the surface potential (surface inversion or accumulation), were affected by both the pre-oxidation treatment and the concentration of certain impurities in the silicon crystal. Furthermore, the resulting surface potential was virtually locked and showed no sensitivity to wet ambients, ammonia vapor or ozone.

iii. *Compatibility.* We have demonstrated the applicability of the oxidation process to certain device structures. We must stress, however, that it cannot be considered as a universal process which can be applied to any arbitrary device structure and maintain some desired surface properties. The oxidation process provides not only a stable surface but a completely new kind of surface with its own characteristic properties. In applying the process to devices, it cannot be considered simply as a stabilization of surface properties but must, instead, be considered as an integral part of the device structure. From this evolves the important concept of "surface design" which should be incorporated in the early stages of device design.

VIII. ACKNOWLEDGMENT

Among the many people who have contributed to this work we wish to thank J. M. Goldey, B. T. Howard and C. A. Bittmann for providing all the diffused silicon junctions; M. Tanenbaum and E. Kolb for the high-purity crystals; A. V. Voinier and G. Reich for the design and construction of the equipment and E. I. Povilonis for processing. We also wish to thank V. O. Mowery for his contributions to the field effect studies, H. Gummel for the noise measurements and Mrs. M. H. Read for the diffraction studies.

REFERENCES

1. Tamm, I., Physik. Z. Sowjetunion, **1**, 1932, p. 733.
2. Shockley, W., Phys. Rev., **56**, 1939, p. 317.
3. Farnsworth, H. E., Schlier, R. E., George, T. H. and Burger, R. M., J. Appl. Phys., **26**, 1955, p. 252.
4. Allen, F., Tech. Rep. 236, Cruft Lab., Harvard Univ., Cambridge, Mass., 1955.
5. Allen, F., Tech. Rep. 237, Cruft Lab., Harvard Univ., Cambridge, Mass., 1955.
6. Dillon, J. A., Bull. Amer. Phys. Soc., **1**, 1956, p. 53; Dillon, J. A. and Farnsworth, H. E., Phys. Rev., **99**, 1955, p. 1643.
7. Wallis, G. and Wang, S., Bull. Amer. Phys. Soc., **1**, 1956, p. 52.
8. Madden, H. H. and Farnsworth, H. E., Bull. Amer. Phys. Soc., **1**, 1956, p. 53.
9. Autler, S. H., McWhorter, A. L. and Gebbie, H. A., Bull. Amer. Phys. Soc., **1**, 1956, p. 145.
10. Law, J. T. and Garrett, C. G. B., J. Appl. Phys., **27**, 1956, p. 656.
11. Handler, P., Bull. Amer. Phys. Soc., **1**, 1956, p. 144.

12. Palmer, D. R. and Davenbough, C. E., Bull. Amer. Phys. Soc., **3,** 1958, p. 138.
13. D'Asaro, L. A., J. Appl. Phys., **29,** 1958, p. 33.
14. Allen, F., private communication.
15. Hagstrum, H. D., Bull. Amer. Phys. Soc., **2,** 1957, p. 133.
16. Dillon, J. A., Bull. Amer. Phys. Soc., **3,** 1958, p. 31.
17. Bardeen, J., Phys. Rev., **71,** 1947, p. 717.
18. Brown, W. L., Phys. Rev., **100,** 1955, p. 590.
19. Montgomery, H. C. and Brown, W. L., Phys. Rev., **103,** 1956, p. 865.
20. Garrett, C. G. B. and Brattain, W. H., B.S.T.J., **35,** 1956, p. 1041.
21. Brown, W. L., Phys. Rev., **91,** 1953, p. 518.
22. Statz, H., DeMars, G. A., Davis, L., Jr., Adams, A., Jr., Phys. Rev., **101,** 1956, p. 1272.
23. Garrett, C. G. B. and Brattain, W. H., Phys. Rev., **99,** 1955, p. 376.
24. Kingston, R. H. and Neustadter, S. F., J. Appl. Phys., **26,** 1955, p. 718.
25. Schrieffer, J. R., Phys. Rev., **97,** 1955, p. 641.
26. Wolff, P., private communication.
27. Brattain, W. H., and Bardeen, J., B.S.T.J., **32,** 1953, p. 1.
28. Ligenza, J. R., private communication (to be published).
29. Fuller, C. S. and Logan, R. A., J. Appl. Phys., **28,** 1957, p. 1427.
30. Fuller, C. S., private communication.
31. Taft, E. A. and Horn, F. H., Phys. Rev., **93,** 1954, p. 64.
32. Collins, E. D., Carlson, R. O. and Gallagher, C. J., Phys. Rev., **105,** 1957, p. 1168.
33. Pratt, G. W., Jr., Lincoln Lab. Quart. Prog. Rep., **12,** February 1, 1955.
34. Lax, B. and Neustadter, S., J. Appl. Phys., **25,** 1954, p. 1148.
35. Shockley, W., *Electrons and Holes in Semiconductors,* D. Van Nostrand and Co., New York, 1950.
36. Shockley, W. and Read, W. T., Jr., Phys. Rev., **87,** 1952, p. 835.
37. Pell, E. M., J. Appl. Phys., **26,** 1955, p. 659.
38. Sah, C. T., Noyce, R. N. and Shockley, W., Proc. I.R.E., **45,** 1957, p. 1228.
39. Chynoweth, A. G. and McKay, K. G., Phys. Rev., **102,** 1956, p. 369.
40. Newman, R., Phys. Rev., **100,** 1955, p. 700.
41. Montgomery, H. C., B.S.T.J., **31,** 1952, p. 950.
42. Maple, T. G., Bess, L. and Gebbie, H. A., J. Appl. Phys., **26,** 1955, p. 490.
43. McWhorter, A. L., *Semiconductor Surface Physics,* Univ. of Pennsylvania Press, Philadelphia, 1957.
44. North, D. O., Bull. Am. Phys. Soc., **2,** 1957, p. 319.
45. Bess, L., Phys. Rev., **91,** 1953, p. 1569.
46. Bess, L., Phys. Rev., **103,** 1956, p. 72.
47. Stevenson, D. T. and Keyes, R. J., Physica, **20,** 1954, p. 1041.